

The Relationship between Snow Accumulation at Mt. Logan, Yukon, Canada, and Climate Variability in the North Pacific

SUMMER RUPPER, ERIC J. STEIG, AND GERARD ROE

Department of Earth and Space Sciences, and Quaternary Research Center, University of Washington, Seattle, Washington

(Manuscript received 24 June 2003, in final form 29 January 2004)

ABSTRACT

An ice core from Mt. Logan, Yukon, Canada, presents an opportunity to evaluate the degree to which ice core accumulation records can be interpreted as meaningful measures of interannual climate variability. Statistical analyses and comparisons with synoptic station data are used to identify the physical relationships between Mt. Logan ice core accumulation data and large-scale atmospheric circulation. These analyses demonstrate that only the winters of high accumulation years have a robust connection with atmospheric circulation. There are no consistent relationships during anomalously low and average accumulation years. The wintertime of high accumulation years is associated with an enhanced trough–ridge structure at 500 hPa and in sea level pressure over the northeast Pacific and western Canada, consistent with increased southerly flow bringing in warmer, moister air to the region. While both storm (i.e., 2–6 days) and blocking (i.e., 15–20 days) events project onto the same climate pattern, only the big storm events give rise to the dynamical moisture convergence necessary for anomalous accumulation. Taken together, these results suggest that while the Mt. Logan accumulation record is not a simple record of Pacific climate variability, anomalously high accumulation years are a reliable indicator of wintertime circulation and, in particular, of northeast Pacific storms.

1. Introduction

Characterization of natural climate variability is essential to understanding climate change and climate impacts on marine and terrestrial ecosystems, as well as to our ability to predict climate. The short instrumental record, however, makes it difficult to describe climate variability on decadal and longer time scales. Ice cores provide one possible means to extend the climate record into the preinstrumental era. Yet despite their clear utility in providing information about past climate on relatively long (e.g., centennial or millennial) time scales, ice core proxy records are not widely accepted as reliable indicators of climate on shorter time scales. Criticisms include the suggestion that the signal-to-noise ratio is too large and that relationships between measured ice core parameters and conventional climate measurements (e.g., temperature or precipitation) are too poorly constrained or are nonstationary (e.g., Shmutz et al. 2000). Despite such concerns, ice core data have been used in quantitative reconstructions of climate variability at interannual time scales (e.g., Barlow et al. 1993; Mann et al. 1998; Appenzeller et al. 1998). Here, we seek to critically evaluate the statistical and physical

basis for using one such record—a snow accumulation time series from an ice core drilled at Mt. Logan, Yukon, Canada (Holdsworth et al. 1992)—as an indicator of North Pacific climate variability. The Mt. Logan core is of particular interest because of its potential in examining decadal-scale Pacific climate variability, which has recently been highlighted in the literature.

The ice core discussed in this study contains nearly 300-yr records of accumulation (Fig. 1) and stable water isotopes at annual resolution. In addition, a second core at Mt. Logan was drilled to bedrock in 2002 (D. Fisher 2002, personal communication) and is in the process of being analyzed. This second core is expected to contain over 10 000 yr of information. These records were obtained from a region that experiences a large amount of variability associated with the El Niño–Southern Oscillation (ENSO) and the Pacific decadal oscillation (PDO) and is at the end of the North Pacific storm track (e.g., Blackmon 1976; Wallace and Gutzler 1981; Mantua et al. 1997; Moore et al. 2003). Mount Logan is therefore in an area of climatological importance. We use the annual accumulation time series from the first Logan core with the expectation that it reflects regional North Pacific weather. Since interannual weather variations can be related to large-scale climate patterns, accumulation at Mt. Logan is a good candidate for extending our knowledge of North Pacific climate variability. However, these patterns are seasonally variable, with wintertime tending to dominate the overall vari-

Corresponding author address: Dr. Summer Rupper, Department of Earth and Space Sciences, University of Washington, Box 351310, Seattle, WA 98195.
E-mail: sbr3@u.washington.edu

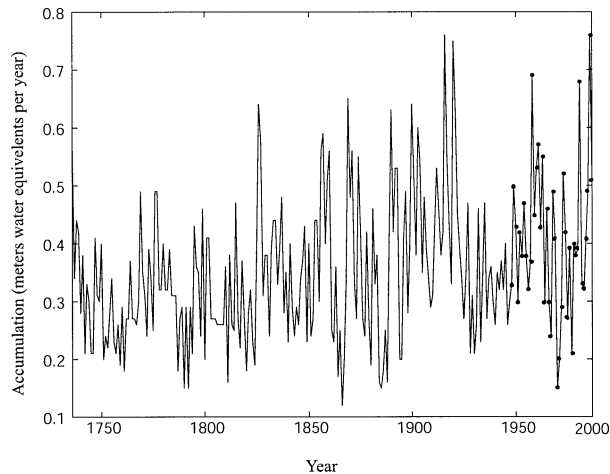


FIG. 1. Annual snow accumulation at the Mt. Logan drill site for 1736–1987. The dotted section corresponds to the years used in this study.

ability. This suggests a possible limitation to the use of ice core accumulation data, for which only full-year averages are available.

Moore et al. (2002a) used comparisons of annual accumulation data at Mt. Logan from 1948 to 2000 with atmospheric variables to infer that during years when accumulation is anomalously high (one standard deviation above the mean), there is increased southerly flow bringing in warmer, moister air than usual. They argue that the reverse is true for anomalously low accumulation years (one standard deviation below the mean accumulation). This is a plausible relationship between large-scale atmospheric circulation and variations in the ice core record. However, the magnitudes of the variations in such annually averaged composite analyses during anomalous accumulation years are small and therefore provide limited insight into the actual physical connection between atmospheric circulation anomalies and variability in the ice core accumulation. Composites of anomalously high accumulation and winter (January–February–March) averaged atmospheric circulation patterns reported by Moore et al. (2003) are similar to the annually averaged composites. The winter averaged atmospheric anomalies during anomalously high accumulation years are much larger and are a strong indication that seasonal breakdowns of the data are likely important.

Attempts have also been made to establish the physical relationships between large-scale atmospheric circulation and glacier mass balance records in the North Pacific (e.g., Walters and Meier 1989; Hodge et al. 1998; Bitz and Battisti 1999). In particular, Bitz and Battisti (1999) examined the relationship between geopotential heights and the winter mass balance of several Pacific Northwest and Alaskan glaciers. They analyzed this relationship further through comparisons with precipitation station records and maps of storm track activity.

Their results suggest that increases in winter mass balance in Washington and British Columbia maritime glaciers correlate with increases in storminess. Variations in winter mass balances in Alaska, on the other hand, were attributed to changes in average moisture flux to the region. This is corroborated by the results of Moore et al. (2002a, 2003), as might be expected given the proximity of Mt. Logan to the Alaskan records. It is important to note, however, that the two types of records are not strictly comparable because winter mass balance incorporates the influence of changes in area and surface elevation (e.g., Elsberg et al. 2001), while the Logan ice core record is a site-specific measurement. Nevertheless, the favorable comparison provides motivation for further analysis of the Logan record, since it has the potential to provide a much longer record than is available from glacier mass balance data.

In this paper, we explore the relationship between the Mt. Logan accumulation data and atmospheric circulation with an emphasis on the contribution of season-specific anomalies to the annual mean accumulation record. In particular, we employ composite techniques to identify physical relationships between the interannual variability in the Logan core and atmospheric circulation variables on seasonal time scales. We show that variability in the Mt. Logan accumulation is associated with wintertime circulation and that only anomalously high accumulation years are diagnostic of atmospheric conditions. To investigate this relationship further we compare the seasonal composites to daily circulation patterns and precipitation station data. This allows for the identification of individual storm events and daily atmospheric circulation patterns that cumulatively produce the time-averaged annual accumulation. This is essential to understanding what atmospheric factors are actually recorded by the accumulation time series, which in turn is critical in assessing how variability in the Logan accumulation relates to North Pacific climate indices [such as the Pacific decadal oscillation and the Pacific North American (PNA) pattern] and whether these data contain reliable information regarding North Pacific climate variability. Comparisons between composite patterns and daily anomaly patterns and precipitation records provide evidence that anomalous accumulation is associated with individual storms and not simple moisture flux associated with increased large-scale circulation.

2. The Mt. Logan ice core

Mount Logan is located in the heavily glaciated St. Elias range on the border of the Yukon and Alaska and is the highest peak in Canada (5957 m above sea level; Fig. 2). The main ice core was drilled in 1980 on a broad saddle at 5340 m above sea level and extended down to 103 m (Holdsworth et al. 1992). Later, shallow coring and snow pit sampling was used to extend the record first to 1987 and later to 2001. The age versus

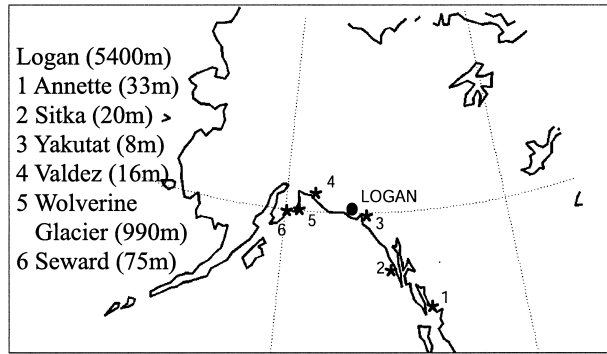


FIG. 2. Map of Alaska and part of the Yukon showing the locations and elevations of the Mt. Logan ice core (dot) and precipitation stations (stars).

depth relationship was established with various visual stratigraphic techniques, including seasonal $\delta^{18}\text{O}$ and nitrate variations, bomb-tritium, and identification of volcanic events of known age [see Holdsworth (1986), Holdsworth et al. (1992), and Whitlow et al. (1994) for a more detailed description of the extraction and dating of the core]. We do not use the 1988 to 2001 data here because the seasonal $\delta^{18}\text{O}$ signals (E. J. Steig and S. Rupper 2002, unpublished manuscript) are indistinct and suggest significant uncertainty in the age–depth relationship. We use the section of the core that overlaps with the National Centers for Environmental Prediction–National Center for Atmospheric Research (NCEP–NCAR) reanalysis data (Kalnay et al. 1996).

Accumulation at the Mt. Logan core site is not affected by summer melting and is therefore expected to be a reliable record of annual snow accumulation that can be related directly to annual precipitation totals. As is true with any core, however, certain factors can complicate this relationship. For example, dating errors can be an issue, especially in sections of ice cores that are not close to reference horizons. However, the identification of a significant relationship with atmospheric circulation here and in Moore et al. (2002a, 2003) is strong support that the depth–age relationship is reliable in this core. Also, because the density of the firn¹ increases with depth, uncertainty in density measurements will contribute to uncertainty in net water-equivalent accumulation. At greater depth, ice deformation and flow cause thinning of annual layers. Holdsworth et al. (1992) corrected for layer thinning using vertical strain rates calculated from measurements of borehole tilt and inclination of visible layers and modeled flow trajectories from a 2D finite element ice flow model. The estimated errors in accumulation measurements (Holdsworth et al. 1992) are negligible relative to the interannual variability, generating confidence that accumulation reflects year-to-year variations. In addition, although errors in

these calculations could introduce a spurious trend to the accumulation data, this would have a relatively small impact on the 40-yr record analyzed in this paper, which is based only on the upper 25 m of the 103-m-deep core.

Other nonsystematic errors may also exist but are harder to correct for. For example, surface sastrugi² evident at the core site and in the borehole (Holdsworth et al. 1992) suggest that accumulation may be affected by winds redistributing snow in the area. Some of the effects of wind are taken into account by the correction for observed tilt in firn layering (as noted above), but it is more difficult to account for large amounts of surface erosion or deposition due to very high winds. Avalanching from the upslope areas of the saddle has also been suggested as a possible source of error. However, there is no evidence of avalanches reaching the interior of the saddle area where this core was drilled.

In summary, errors may arise from dating and density measurement errors, ice deformation and flow, wind and avalanching affects, as well as other elements giving rise to local noise in the core. While these various sources are difficult to quantify, results from previous studies and the results we present here suggest that the Logan core provides a reliable record of accumulation, at least for the period of interest in this study (Holdsworth et al. 1992; Moore et al. 2002a,b).

We now seek to understand the variability in accumulation and to identify the relationship between this variability and the large-scale atmospheric circulation. The power spectrum estimate for the Logan time series (windowed periodogram, Hanning window, 10 degrees of freedom), which is shown in Fig. 3, highlights the redness of the spectrum. Much of the variance in the record occurs at periods of ~ 10 yr and longer, reflecting the decadal variability seen by inspection of the time series. Also shown in Fig. 3 is the best-fit first-order autoregressive process [AR(1) or “red noise”], together with its 95% confidence limits (e.g., Jenkins and Watts 1968; Schneider and Neumaier 2001). That the Logan spectral estimate lies largely within the 95% confidence limit is a strong suggestion that the time series is well described by an AR(1) process, although we note that using a different spectral method, Moore et al. (2001, 2003) identify a significant peak at ~ 3.8 yr, which they argue reflects the influence of the El Niño–Southern Oscillation.

The coefficients in an AR(1) process can be identified with a characteristic physical time scale (e.g., Jenkins and Watts 1968), which represents the e -folding time for relaxation of the system back to its equilibrium state. For the best-fit AR(1) process to the Logan core, this is $\sim 0.8 \pm 0.3$ yr (95% confidence limits; e.g., Schneider and Neumaier 2001) and as such is consistent with an annual time scale. While an AR(1) process can account for all of the variance in the accumulation record, it is

¹ Material in the intermediate stages of transformation from snow to ice (e.g., Paterson 1994)

² Elongated erosional ridges on the snow surface resulting from wind.

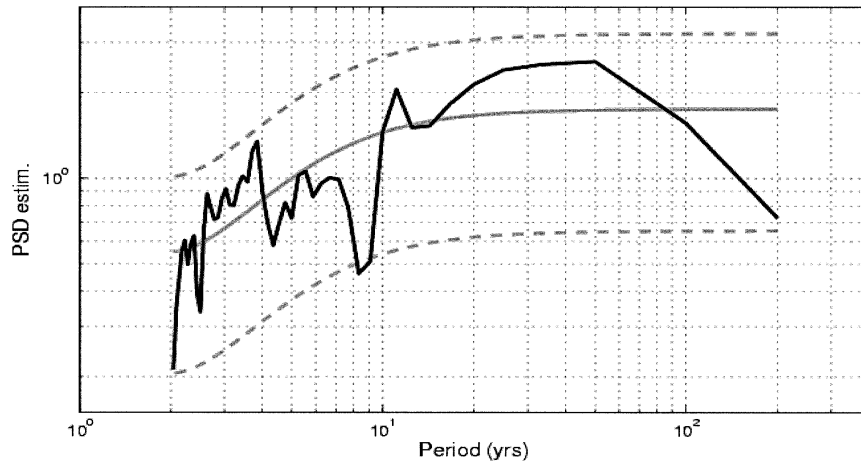


FIG. 3. Mt. Logan accumulation time series, power spectrum, and red noise model. Power spectrum density (PSD) estimate for the accumulation using a windowed periodogram, Hanning window, and 10 degrees of freedom on a log log plot (black curve). The best-fit first-order autoregressive process is the solid gray line with the 95% confidence limits (dashed gray lines).

not quite a self-consistent explanation of the time series. After removing the autocorrelations from the time series, the residuals are not consistent with random, normally distributed white noise, which is one of the AR(1) process assumptions (e.g., Jenkins and Watts 1968). Instead, the distribution of the residuals is slightly skewed toward positive values. This is perhaps not surprising since atmospheric moisture is a nonlinear function of temperature; due to the Clausius–Clapeyron relation, a normal distribution of random temperatures would give rise to a positively skewed distribution of moisture (for a fixed relative humidity).

The same skewness is also seen in a histogram of the actual accumulation values (Fig. 4). This is intriguing as it suggests that anomalous years may be especially important. It also suggests that, due to the non-Gaussian properties of the time series, anomalous years used for composite analysis may be better computed based on the histogram and not one standard deviation above and

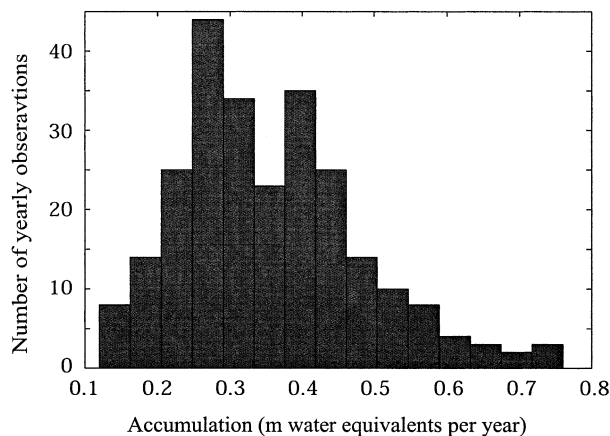


FIG. 4. Histogram of accumulation. Note that the accumulation is positively skewed.

below the mean [as is commonly used in composite analysis (e.g., Moore et al. 2002a)]. We therefore define anomalously high accumulation years to be those with accumulation greater than 0.50 m yr^{-1} (water equivalent; see Table 1). However, we define anomalously low accumulation years to be those with less than 0.28 m yr^{-1} (one standard deviation below the mean) because this gives a sufficient number of years for compositing. (For brevity, we use the phrases “high accumulation” and “low accumulation” as opposed to “anomalously high accumulation” and “anomalously low accumulation” for the rest of the paper.) We will show that low accumulation years, regardless of the number of years used in the composites, do not have a clear relationship with atmospheric variables. Conversely, the pattern in the eight high accumulation years is remarkably robust despite averaging over a large number of years, giving confidence in the results. [We note that the results are inconsistent when the 1987–2001 data is included. Possibly, this indicates that the significant trend in accumulation since 1987, as inferred by Moore et al. (2002b), may require a different inter-

TABLE 1. Anomalously high and low accumulation. High years are defined based on the histogram (Fig. 4). Low years are defined as one standard deviation below the mean.

High accumulation yr	Accumulation m yr^{-1}	Low accumulation yr	Accumulation m yr^{-1}
1958	0.687	1967	0.244
1960	0.532	1970	0.152
1961	0.573	1971	0.202
1963	0.551	1975	0.272
1973	0.525	1977	0.211
1981	0.680		
1986	0.760		
1987	0.510		

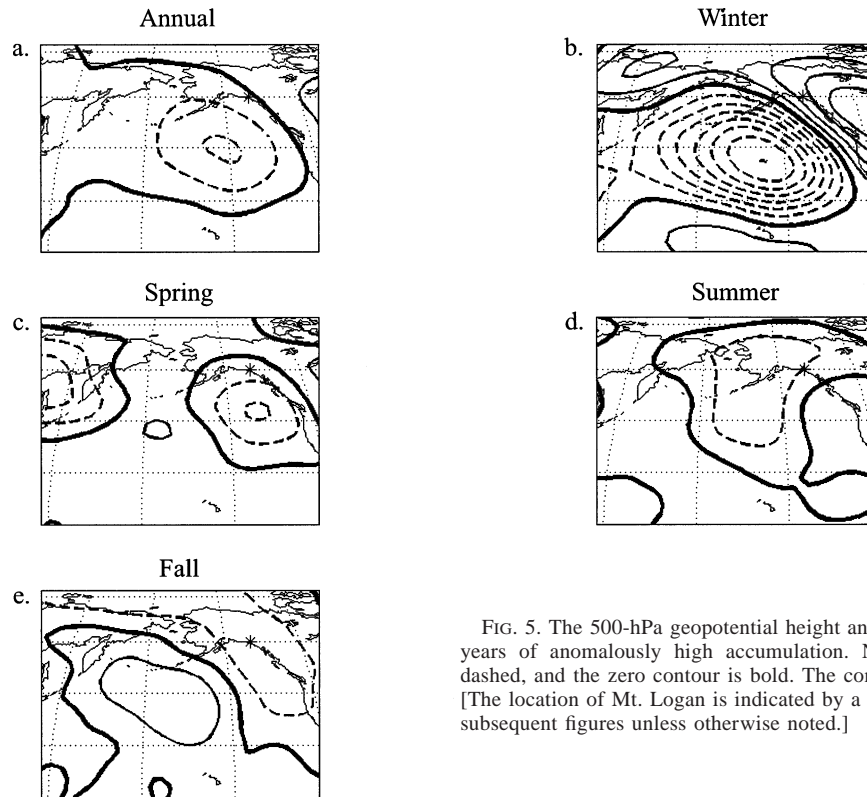


FIG. 5. The 500-hPa geopotential height anomalies averaged over years of anomalously high accumulation. Negative contours are dashed, and the zero contour is bold. The contour interval is 10 m. [The location of Mt. Logan is indicated by a star (*) here and in all subsequent figures unless otherwise noted.]

pretation than the interannual variability in accumulation discussed here. However, as noted in the introduction, we do not consider the accuracy of the dating in this section of the core to be reliable enough for annual composite analysis.]

3. Relationship between atmospheric circulation patterns and accumulation

We use composite analysis to examine the relationship between accumulation at Mt. Logan and the atmospheric patterns giving rise to it. As noted in the introduction, we only have annual average accumulation data. Therefore, it is natural to begin the compositing analysis using annual averages. We investigate the relationships in more detail with seasonal composites (later in this section) and daily data (section 4).

a. 500-hPa geopotential height anomaly composites

The 500-hPa geopotential height anomaly (Z_{500}) annual composites for anomalously high and low accumulation years (as defined above) are shown in Figs. 5a and 6a. These composites are based on the NCEP–NCAR reanalysis datasets of 2.5° gridded data (Kalnay et al. 1996). The 500-hPa geopotential heights were selected, not only because they provide important information on the midtroposphere atmospheric circulation in the Pacific and the strength and position of the jet

stream, but also because the 500-hPa level is situated close to the same elevation as the drill site. During high accumulation years, the Z_{500} are anomalously low over the North Pacific and anomalously high over Canada (Fig. 5a). The reverse is true during low accumulation years: the Z_{500} are anomalously high over the North Pacific and anomalously low over Canada (Fig. 6a). These results broadly reproduce the annual composite patterns reported by Moore et al. (2002a). However, it is not clear how to interpret an annual mean composite, as this region experiences a large amount of seasonal variability. Moreover, the amplitude in the atmospheric circulation anomaly (order of 20 m) is only associated with a weak circulation pattern. We therefore turn to seasonal composites to determine if a meaningful relationship between atmospheric circulation and annual accumulation exists.

Seasonal composites of Z_{500} during high accumulation years are shown in Figs. 5b–e. The winter (December–January–February) anomaly pattern (Fig. 5b) is similar to the annual pattern (Fig. 5a), with a broad anomalous low over the North Pacific and an anomalous high over Canada. However, the wintertime composite exhibits variations in height anomalies 4 times larger than in the annual composite [consistent with the results presented by Moore et al. (2003)]. Also, the centers of action are statistically different from the seasonal mean at the 95% significance level (by the Student's t test). This implies that the physical relationship between accumulation and

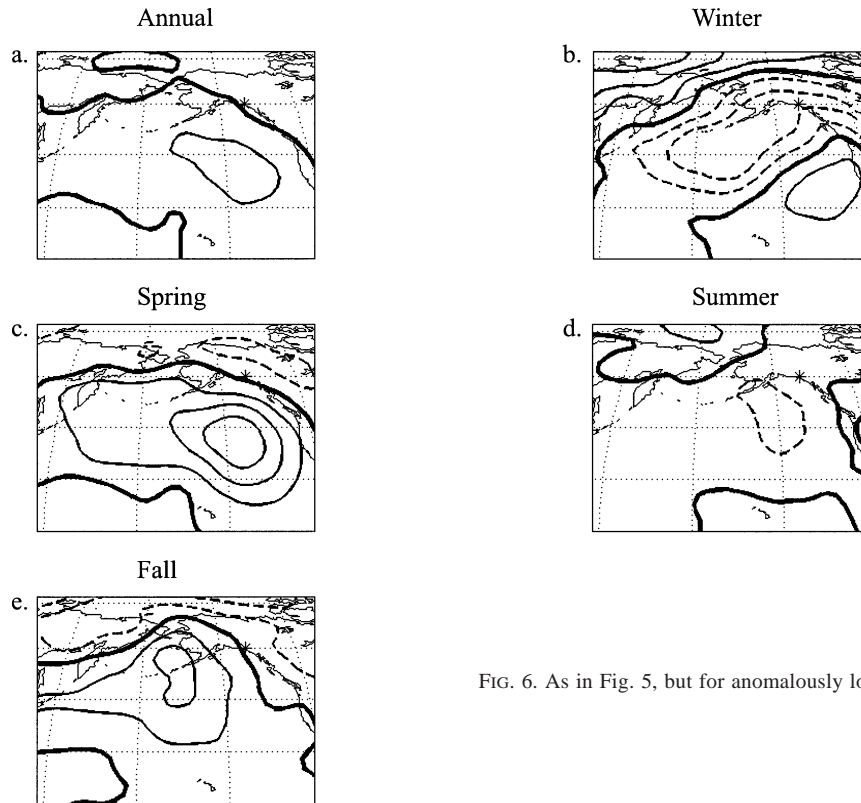


FIG. 6. As in Fig. 5, but for anomalously low accumulation years.

atmospheric circulation is essentially a wintertime phenomenon. This is confirmed by the fact that the Z_{500} spring, summer, and fall composites (Figs. 5c–e) do not show large anomalies and are not statistically different from the mean. Also, subsampling of the data into individual years (discussed below) shows that only the wintertime patterns are robust. Taken together, these analyses suggest that high accumulation is associated in part with increased southerly flow into Alaska and southwestern Canada during the winter season. We will show in sections 4 and 5 that an increase in storminess is also essential.

The Z_{500} seasonal composites for low accumulation years are displayed in Figs. 6b–e. None of these composites have amplitudes as large as those during high accumulation years, nor are they significantly different from the mean. Also, the seasonal composites during low accumulation years are not stable to subsampling of the data.

The robustness of the seasonal composites can be evaluated by looking at the patterns for each anomalous year. As can be seen in Fig. 7, all wintertime patterns for anomalously high years except for two (1963 and 1973) show broadly the same pattern as the wintertime composites in Fig. 5b. The 1963 pattern is similar to the wintertime composite, but shifted farther south. The monthly anomaly patterns indicate that the Februaries of 1963 and 1973 have strong circulation patterns very similar to the high accumulation wintertime composite,

suggesting that most of the anomalous accumulation may be occurring in February and not December or January for these two years. (Refer to section 5 for additional discussion.) Since six of the eight years are similar, we consider the wintertime composite to be significant. However, for the spring, summer, and fall of high accumulation years and for all of the seasons during low accumulation years (Fig. 8; only winter is shown for brevity), the patterns are highly variable (Figs. 5c–e and 6b–e). This indicates that there are several possible atmospheric circulation patterns that result in average and low accumulation but only one consistent pattern associated with high accumulation. Thus the overall picture from the composite analysis suggests a nonlinear relationship between accumulation and atmospheric circulation patterns; high accumulation years are the only years diagnostic of any particular pattern of atmospheric circulation. This is in contrast with the results of Moore et al. (2002), where only annual averages are diagnosed and the low accumulation years are considered robust.

b. Sea level pressure anomaly composites

The 500-hPa geopotential heights discussed above are next compared to sea level pressure (SLP) composites (Figs. 9 and 10) to compare the surface anomalies to anomalies at midlevels. Surface pressure in the North Pacific and Gulf of Alaska is often characterized by the strength of the Aleutian low pressure system. The Aleu-

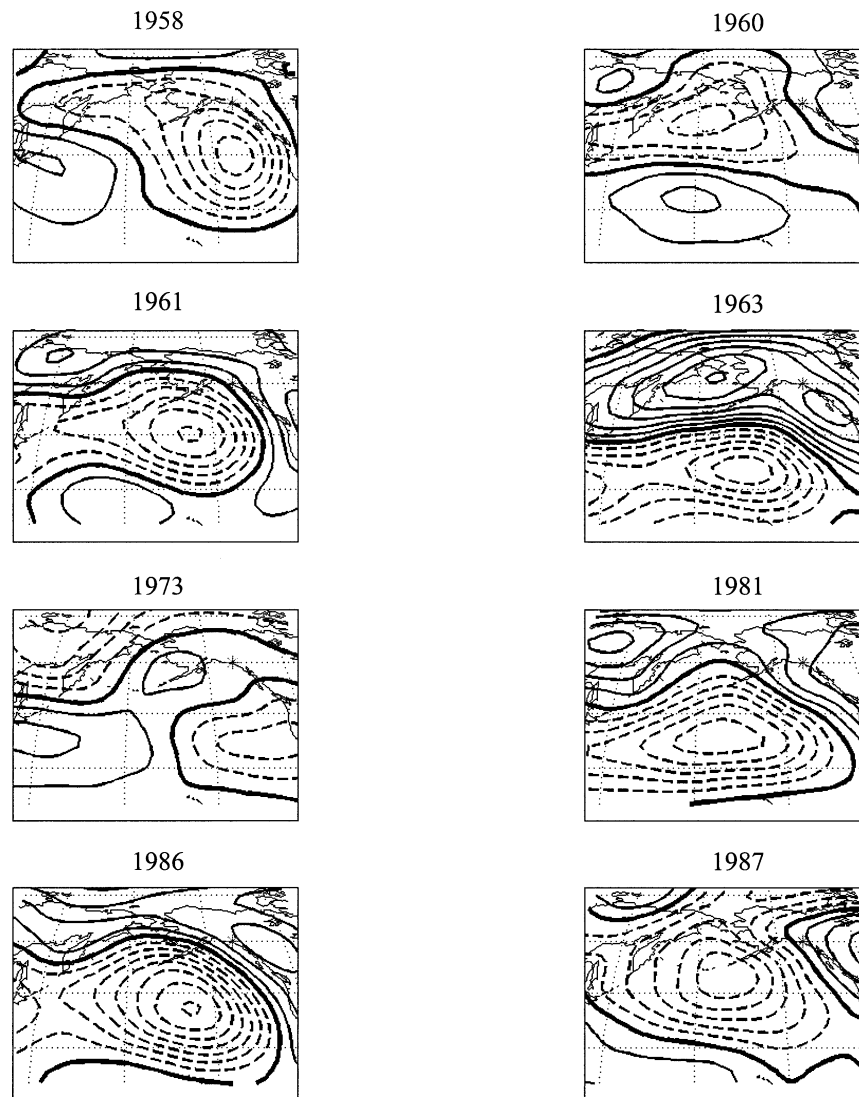


FIG. 7. The 500-hPa geopotential height anomalies for each of the anomalously high accumulation years. The contour interval is 20 m. The zero contour is bold, and the negative contours are dashed. Note that 1963 and 1973 are the most different.

tian low, centered in the North Pacific around the Aleutian Islands, is strongest in the winter and all but disappears in the summer. The position and intensity of the Aleutian low pressure center has been taken as an important measure of the strength of storms in areas around the Gulf of Alaska and the Pacific Northwest (e.g., Trenberth and Hurrell 1994; Beamish et al. 1997; Overland et al. 1999). Since the Z_{500} composites were strongly linked to the winter conditions and the Aleutian low pressure center is strongest in the winter, we expect that wintertime SLP anomaly composites will be the most important.

A deeper eastward-shifted low pressure anomaly is evident in the composite of annual SLP anomalies during high accumulation years (Fig. 9a). The reverse relationship is apparent in the annual SLP anomalies dur-

ing low accumulation years (Fig. 10a). However, as with the annual Z_{500} composites, these anomalies are weak, and the seasonal patterns (discussed below) are significantly more convincing.

The wintertime composite of SLP anomalies for high accumulation shown in Fig. 9b has a similar anomaly pattern to the annual pattern, but with a magnitude 5 times greater than that of the annual composites. SLP anomaly patterns during spring, summer, and fall (Figs. 9c–e) are not as large as the winter anomalies, as is the case for summer and fall of the low accumulation years (Figs. 10b–e). Though winter and spring of low accumulation years have patterns that are large in magnitude, subdividing the data into individual years and testing whether these patterns are statistically different from the mean showed that only wintertime circulation during

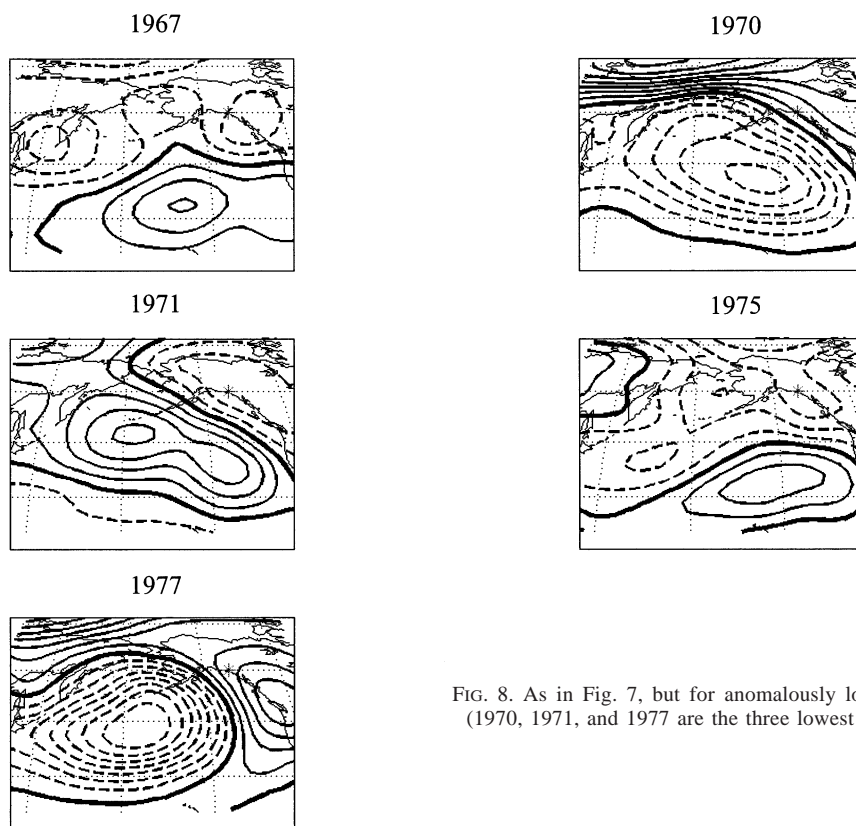


FIG. 8. As in Fig. 7, but for anomalously low accumulation years (1970, 1971, and 1977 are the three lowest accumulation years).

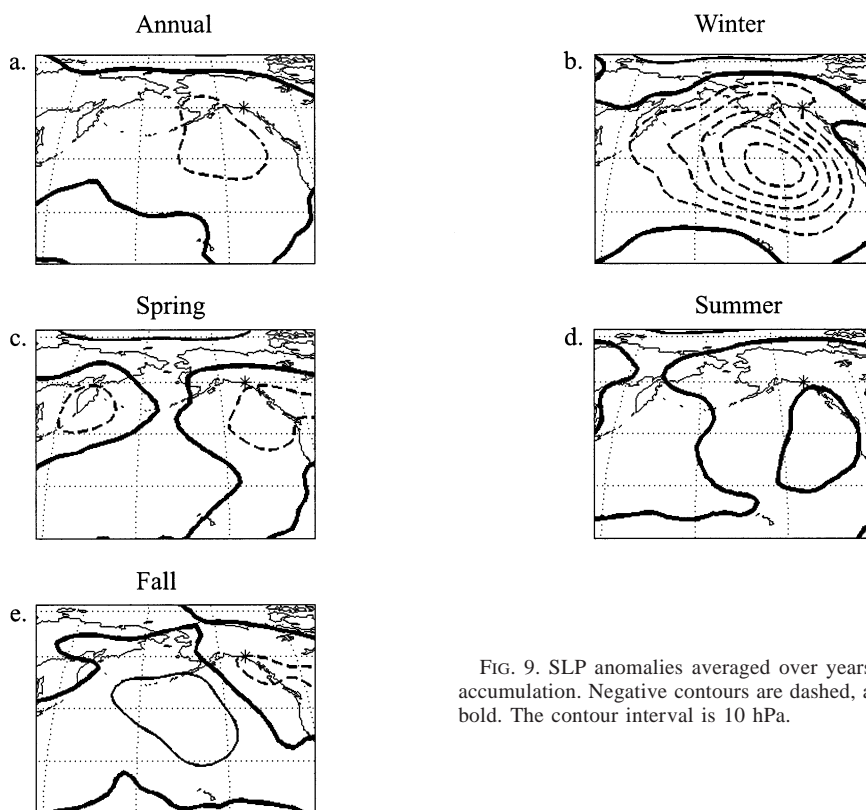


FIG. 9. SLP anomalies averaged over years of anomalously high accumulation. Negative contours are dashed, and the zero contour is bold. The contour interval is 10 hPa.

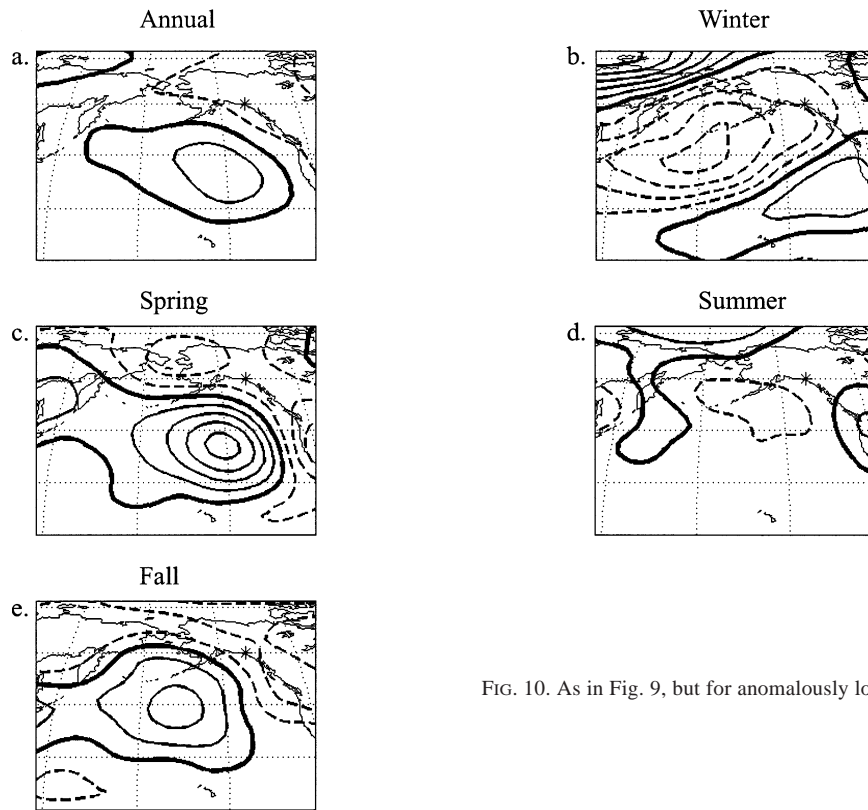


FIG. 10. As in Fig. 9, but for anomalously low accumulation years.

high accumulation years is robust. All other seasons were highly variable from year to year and are not statistically different from the mean at a 95% significance level.

The SLP results largely mirror those for the Z_{500} composites and reinforce the conclusion that only high accumulation years are diagnostic of atmospheric conditions, that there is a nonlinear relationship between atmospheric conditions and accumulation, and that the variability in accumulation at Mt. Logan is associated with variations in wintertime conditions. This is consistent with the Aleutian low pressure system being strongest in the winter.

The enhanced trough–ridge structure in 500-hPa heights and sea level pressure over the Northeast Pacific and western Canada during the winter of high accumulation years is reminiscent of the Pacific North American pattern (e.g., Wallace and Gutzler 1981; Moore et al. 2001). However, it is not clear if the above identified relationship is better thought of as a PNA-like shift in the jet stream or as the result of individual storms and atmospheric blocking events (Lindzen 1986). Furthermore, it may be interesting to note that, while the most distinct relationship with large-scale atmospheric circulation is during the winter season, precipitation in the region around Mt. Logan is greatest in the fall. Snow depth measurements near the ice core site show peaks in snowfall from August to September of 2001 and from January to February of 2002 (D. Fisher, personal com-

munication). The first peak agrees with the fall maximum in precipitation at the weather stations. As more data is collected, it will be interesting to see if this second peak is an anomaly or if it represents normal conditions for high elevations in this region.

4. Storms

We now examine how storminess may contribute to an increase in accumulation under the atmospheric conditions previously identified. This is approached in two ways. First, we seek to determine how the day-to-day variability in large-scale atmospheric conditions combines to create the seasonal means associated with high accumulation that were identified in section 3. This breakdown provides a means for distinguishing between storms in the region around Mt. Logan, atmospheric blocking, and shifts in the season-long mean circulation. Second, we present daily precipitation data at stations near Mt. Logan as evidence that this region experiences additional dynamical convergence in association with anomalously high precipitation (section 5).

We calculate a “pattern index” as the covariance between the Z_{500} wintertime composite pattern for high accumulation years (Fig. 5b) and the daily Z_{500} anomaly values throughout each year. A high value of this index means that the Z_{500} anomaly pattern closely resembles the high accumulation composite anomaly pattern. Daily Z_{500} anomalies are calculated by subtracting the mean

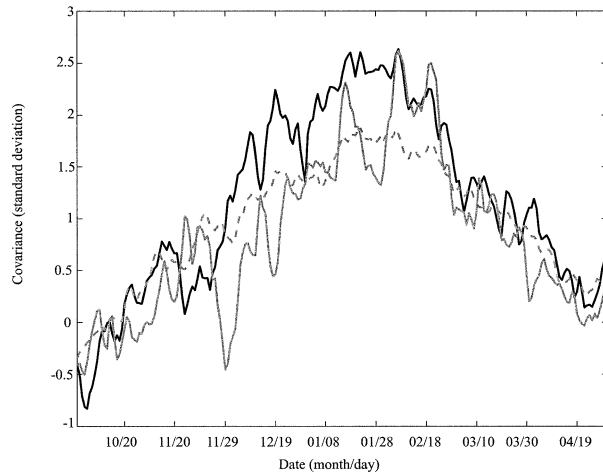


FIG. 11. The curves represent the average standard deviation of the PI (covariance) for high accumulation (solid black), low accumulation (solid gray), and average accumulation (dashed gray) years, from 1 Oct to 30 Apr. See text for details.

wintertime Z_{500} values of all years from the daily Z_{500} values. For example, the wintertime daily 500-hPa geopotential height anomalies for 1 January are equal to the pattern for that day minus the average wintertime 500-hPa heights from 1948 to 1987. These daily Z_{500} patterns are projected onto the wintertime Z_{500} composites for high accumulation years. This results in a pattern index (PI) time series indicating the extent to which each day looks like the winter anomaly composite.

The average PI for all high accumulation years is greater than the average for all years while the average PI for low years is difficult to distinguish from the mean (Fig. 11). This is a further indication that the relationship between extreme years and atmospheric conditions is nonlinear. While in high accumulation years there are 62 days per winter that are one standard deviation above the mean, there are only 15 such days during low accumulation years.

There are also some intriguing details within this index that give further insight into the atmospheric conditions on a day-to-day basis. Figure 12 is an enlarged view of the wintertime PI for 1987, an example of one of the high accumulation years. This particular example year was chosen because, though it has the lowest accumulation of the eight high accumulation years, the results are still very compelling. This is another indication that our method of selecting anomalous years based on the histogram is reasonable. There are obvious sharp peaks as well as broader peaks apparent in the PI for this example year. Peaks that span 2–6 days correspond to a single synoptic storm event while peaks that persist for longer than this are representative of an atmospheric blocking pattern (e.g., Lindzen 1986). To demonstrate this, we present daily sea level pressure and surface temperature maps during one of the 2–6-day storm events (Fig. 13) and one of the blocking

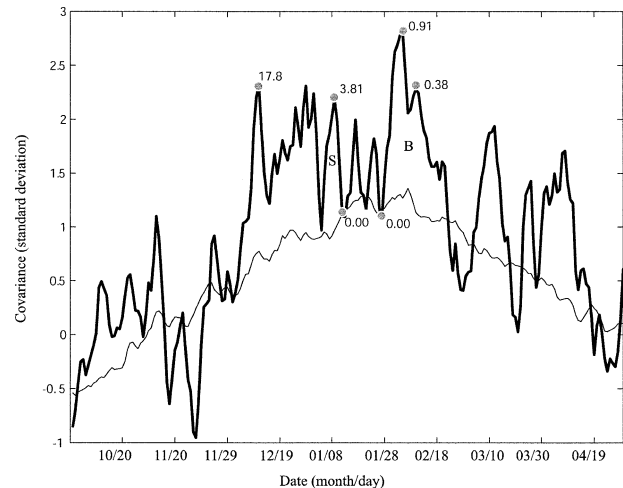


FIG. 12. Standard deviation of the PI during the 1987 anomalously high accumulation year (bold line), average PI for 1948 to 1987 (thin line), and Yakutat total daily precipitation (cm) for selected days along the 1987 PI curve (gray dots). The 2–6-day peaks correspond to storm events (example marked “S”), while broader peaks represent atmospheric blocking (example marked “B”; see Figs. 13 and 14).

events (Fig. 14). The 8 January storm event coincides with a low pressure system that moves across the Pacific into the Gulf of Alaska. Surface temperatures also increase in the Mt. Logan area during this event. Thus, the large-scale composite pattern identified earlier is associated with the evolution of storms in the North Pacific. This is initial evidence that high accumulation corresponds to storm events. During the February blocking event, a low pressure system builds in from the west and then remains relatively stationary around the Aleutian Islands from 2 to 18 February (Fig. 14). The importance of the storm events versus these blocking events will be further examined in the next section.

5. Comparison with station records

Since there are no long records of daily precipitation available for Mt. Logan, it is difficult to assess the relationship between the PI and actual precipitation events. However, if a clear relationship exists between accumulation and nearby precipitation station records, these stations can be used to evaluate daily variability in precipitation in the Mt. Logan region. Direct correlations between the Mt. Logan accumulation and weather station precipitation records, as well as composite analysis of the station records, are used to determine the usefulness of these stations.

a. Precipitation station records

Direct correlations between Mt. Logan and precipitation stations in the region are low and not at all consistent (Table 2; Fig. 2). This is perhaps not surprising as other studies have shown that Alaskan glacial mass

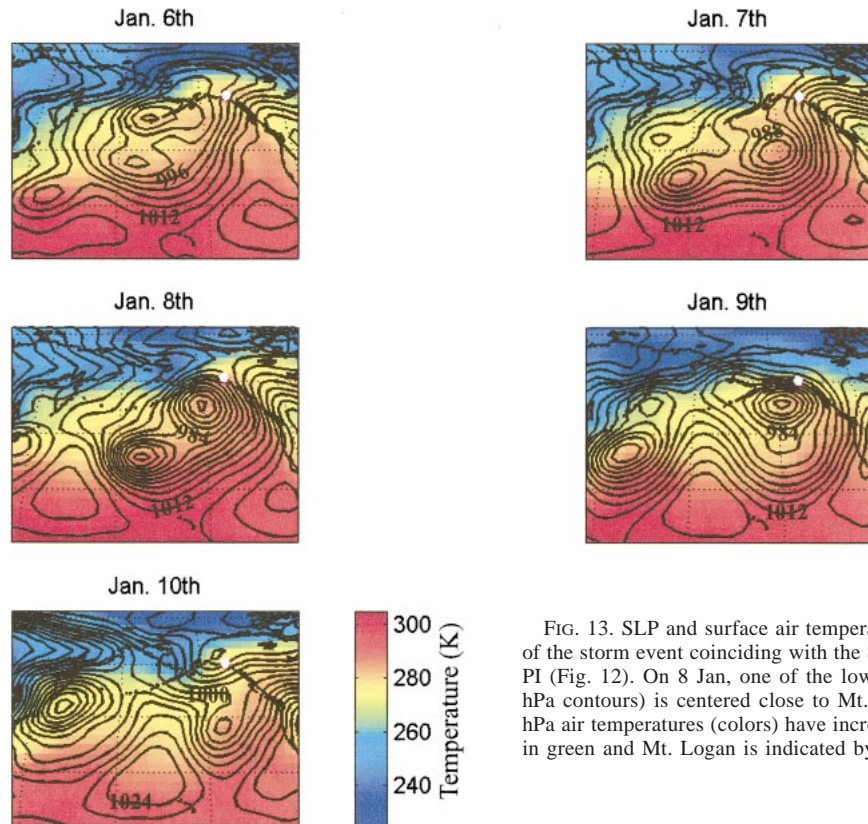


FIG. 13. SLP and surface air temperature for the evolution of the storm event coinciding with the 8 Jan 1987 peak in the PI (Fig. 12). On 8 Jan, one of the low pressure systems (4-hPa contours) is centered close to Mt. Logan and the 1000-hPa air temperatures (colors) have increased. The coastline is in green and Mt. Logan is indicated by the white dot.

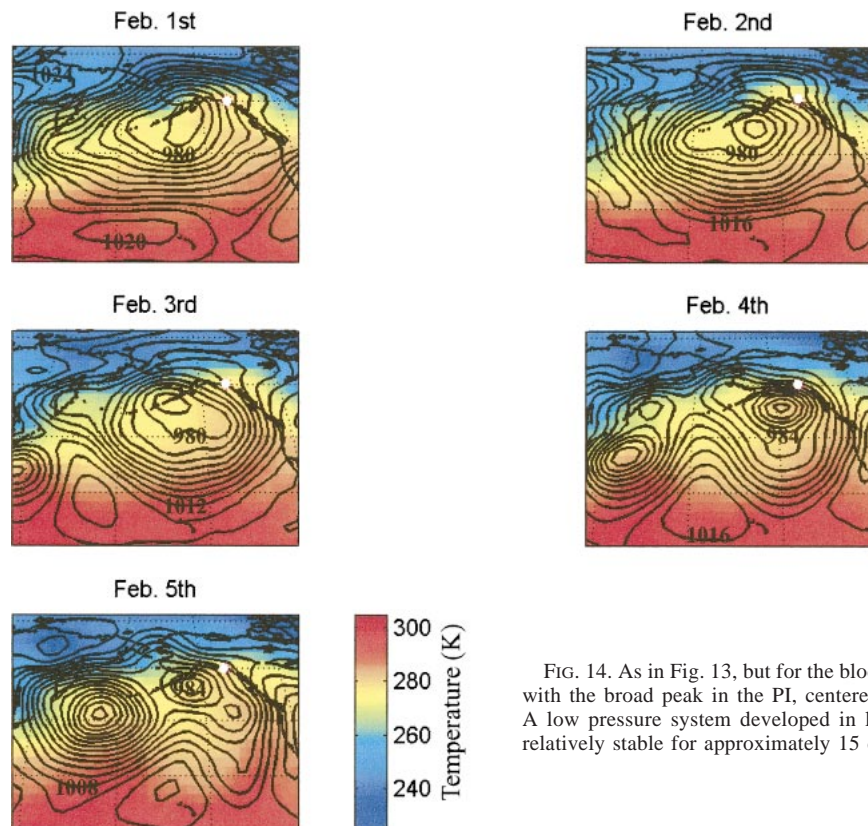


FIG. 14. As in Fig. 13, but for the blocking event coinciding with the broad peak in the PI, centered around 3 Feb 1987. A low pressure system developed in late Jan and remained relatively stable for approximately 15 days.

TABLE 2. Correlation coefficients (r) for the Mt. Logan accumulation and several precipitation station records. The length of each record is in italics, and NA represents two records that did not overlap in time. All precipitation station data sources, except for Wolverine Glacier, are from the National Oceanographic and Atmospheric Administration (updated with data from the World Meteorological Organization). The Wolverine Glacier station data source is the United States Geological Survey. See Fig. 2 for the locations and elevations of each record.

	Logan accumulation	Annette	Sitka	Wolverine Glacier	Yakutat	Valdez	Seward
Logan accumulation	1	-0.38	0.27	-0.08	-0.23	0.09	0.46
Annette		1	0.28	-0.20	0.12	0.03	-0.11
<i>1 Sep 1949–31 Dec 1997</i>							
Sitka			1	-0.08	0.56	0.18	0.31
<i>1 Sep 1949–30 Nov 1996</i>							
Wolverine Glacier				1	-0.09	NA	0.12
<i>Oct 1967–Sep 1998</i>							
Yakutat					1	0.00	0.47
<i>1 Sep 1949–31 Dec 1997</i>							
Valdez						1	0.22
<i>1 Sep 1949–30 June 1964</i>							
Seward							1
<i>1 Sep 1949–31 Oct 1997</i>							

balance records do not correlate very well with local precipitation records (e.g., Bitz and Battisti 1999). Bitz and Battisti (1999) speculate that the local Alaskan precipitation data are not correlated highly with mass balance due to poor quality of the records, the shortness of the records, or regional dependence of the data. However, even records that are thought to be of good quality and reasonable length do not correlate very highly with one another either. This illustrates the significant spatial heterogeneity in precipitation, likely due in part to the complex topography. Thus, the poor correlations among these various records do not necessarily mean they do not relate to large-scale atmospheric circulation in a manner comparable to Logan accumulation. In fact, analyses of the precipitation station records discussed below show that, despite the lack of correlation with the Logan record and the large differences in elevations between the stations and the ice core site, the same large-scale circulation patterns occur during high precipitation years as during high accumulation years.

Compositing is performed on two of the precipitation stations (Yakutat and Sitka, Alaska) in a similar manner to the treatment of the Logan accumulation data presented earlier. The Z_{500} composites (Fig. 15) are calculated based on the anomalously high and low total annual precipitation. As the distribution of precipitation at the surface is more consistent with the Gaussian than the Logan accumulation, we define anomalous precipitation as one standard deviation above and below the mean. As illustrated in Figs. 15a and 15c, there is a distinct relationship between anomalously high precipitation at Yakutat and Sitka stations and large-scale atmospheric circulation during winter. These patterns are very similar to the composites for high accumulation years. Composites during low precipitation years (Figs. 15b,d) show stronger circulation patterns than the composites for low Logan accumulation. This may be a result of the large difference in elevation between the

Mt. Logan ice core and the precipitation stations, suggesting that conditions giving rise to small precipitation events may not occur at higher elevations on Mt. Logan. This could lead to the difficulty in distinguishing low accumulation from average accumulation in the ice core record. It is also possible that the difference between the precipitation composites and accumulation composites arises from local noise due to topographic interference and the geometry of cyclones (e.g., Fisher et al. 1985; Zheng et al. 1998). Or, it could also be true, for instance, that noise levels due to regional meteorology may be relatively large during lower accumulation years. We emphasize though that the high accumulation and high precipitation circulation patterns are very similar. This implies that high accumulation at high elevations in the St. Elias range is controlled by the same factors controlling high precipitation at lower elevations. It also suggests that high accumulation at Mt. Logan is as reliable an indicator of large-scale atmospheric circulation as high precipitation at meteorological stations.

Additional composite analysis is used to further illustrate the relationship between big storms and high accumulation. Wintertime composites of Z_{500} during the high precipitation years averaged only over those days with more than 2.5 cm of rain at Yakutat station showed similar circulation patterns to Figs. 15a,c (high precipitation wintertime composite), but with increased strength in the circulation. This suggests that precipitation is associated with these large-scale patterns. We also used Yakutat precipitation to select days for compositing during the eight high accumulation years (listed in Table 1). Again, the patterns were similar to the wintertime composite (Fig. 5b), but with increased circulation. The year 1963 (which had a different pattern from the other years; discussed in section 3; Fig. 7) does show a similar pattern when composited based on precipitation. The year 1973 does not show similar cir-

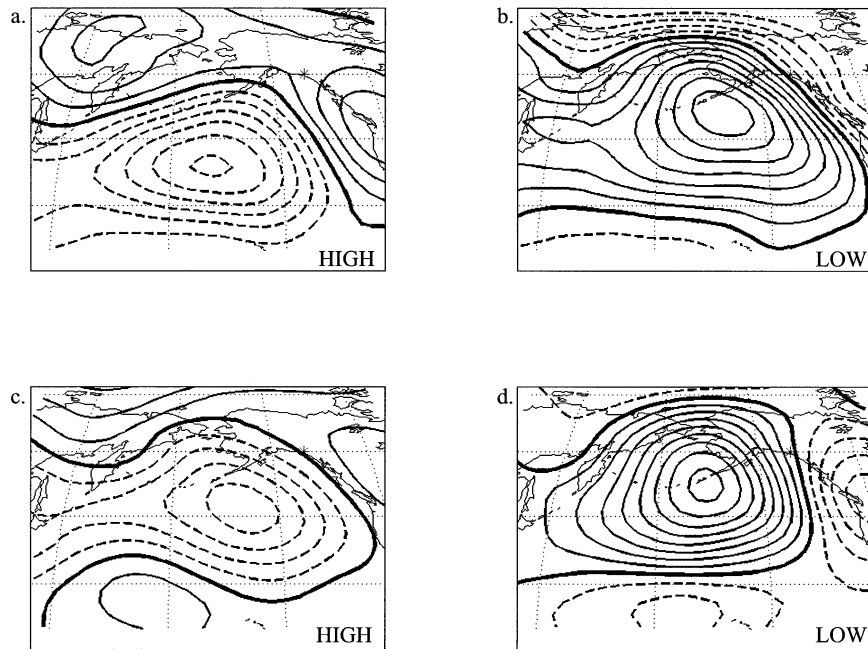


FIG. 15. Wintertime 500-hPa geopotential height anomalies averaged over years of anomalously (a) high and (b) low precipitation at Yakutat station and anomalously (c) high and (d) low precipitation at Sitka station. Negative contours are dashed, and the zero contour is bold. The contour interval is 10 m. Panels (a) and (c) are broadly similar to the winter composite during anomalously high accumulation at Logan (Fig. 5b).

culation even when composited only on days with rainfall. However, the result that seven out of eight of the years are consistent suggests that the relationship between large-scale circulation patterns and anomalously high accumulation can be considered robust.

With a link between the Logan accumulation record and station precipitation established, we can now compare the PI presented in section 4 with records of total daily precipitation. We use the Yakutat precipitation record (total precipitation per day) for this comparison because this station is closest to Mt. Logan (note, however, that the elevation difference between Yakutat and the ice core site is large). Even though Yakutat may not experience anomalous precipitation during the same years that Mt. Logan has anomalous accumulation, large storm or blocking events should affect both sites. A comparison between the 1987 daily PI and 1987 daily precipitation shows that during the 2–6-day storms (the sharp peaks), it is raining at Yakutat station. As an example, the sharp peaks centered around 10 December and 8 January of 1987 correspond to 17.8 cm and 3.8 cm (respectively) of rain at Yakutat (Fig. 12). The blocking events, however, do not appear to correspond with much precipitation. In fact, the highest covariance during the 1987 winter season occurs between 2 and 18 February, one of the blocking events. Even though this period corresponds to a large-scale atmospheric pattern very similar to the wintertime composite during high accumulation years at Mt. Logan, very little rain (less than 1 cm) is associated with it at Yakutat. This is ev-

idence that it is transient storms that result in high accumulation.

b. Yakutat precipitation

Since the same conditions necessary for extreme precipitation at Yakutat are necessary for extreme accumulation at Logan (as discussed in section 4), it is reasonable to use Yakutat precipitation as an indicator of the factors controlling storms at the Mt. Logan core site during fall versus winter. The largest amount of precipitation occurs during the fall (September–October–November; Fig. 16). This implies that precipitation at high elevations on Mt. Logan is also largest in the fall. Why then is variability in accumulation at Mt. Logan and precipitation at Alaskan stations so strongly related to wintertime conditions?

One way to address this issue is to calculate the daily averaged maximum precipitable water (MPW; Peixoto and Oort 1992). If precipitation in a given day exceeds the MPW in the atmospheric column, then there must have been moisture convergence into the air column either through upslope flow, dynamical convergence, or evaporation. Relative humidity (RH; %), combined with air temperature (T_a ; K), can be used to estimate the precipitable water (w ; cm) (e.g., Jensen et al. 1990; Rosenberg et al. 1990):

$$w = \{(0.439 \times \text{RH} \times 0.01) \times \exp[26.23 - (5416 \times T_a^{-1})]\} \times T_a^{-1}. \quad (1)$$

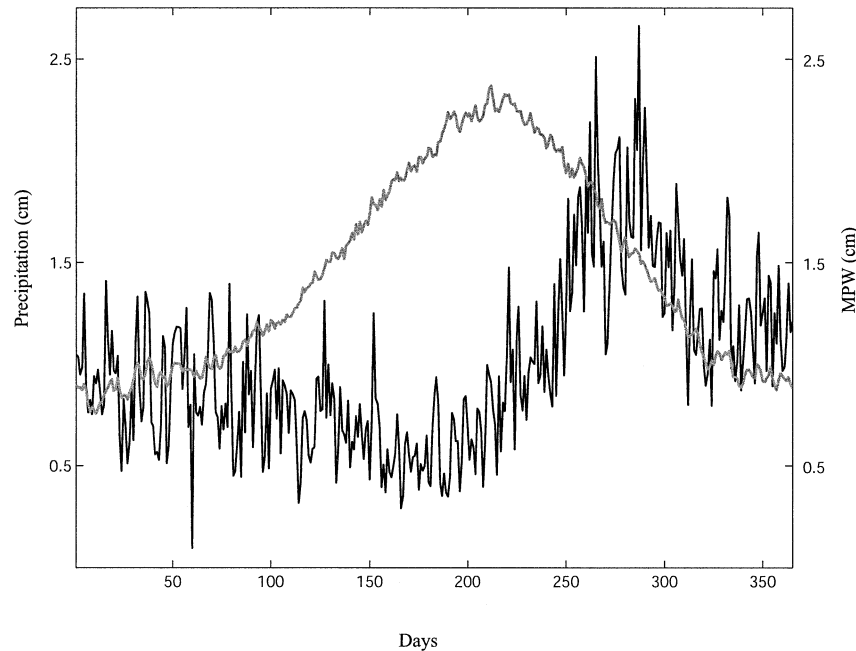


FIG. 16. Yakutat average total daily precipitation (1949–97) (black) and mean MPW (gray). Note that the fall and winter average daily precipitation follow the MPW curve, suggesting that the difference between precipitation in the fall and winter is controlled predominantly by temperature. Day 1 corresponds to 1 Jan.

To calculate the MPW at Yakutat, we substitute mean daily temperature for T_a and RH equal to 100% in the above equation. The results are shown in Fig. 16 as the daily average MPW versus the mean total daily precipitation. Several important features are apparent. First, mean daily precipitation at Yakutat station during spring (March–April–May) and summer (June–July–August) is well below MPW. Fall and winter precipitation is interesting as it follows the shape of the MPW curve but is above MPW. This overall shape suggests that the difference in precipitation between fall and winter is controlled predominantly by the trend in temperature [and not a southward migration of the jet stream (Nakamura 1992; Chang et al. 2002)]. It is also evidence that precipitation during the winter reflects dynamical convergence of moisture in the region.

Furthermore, the average MPW is higher during anomalously high precipitation years than in anomalously low precipitation years. Despite the higher MPW, precipitation still exceeds MPW 40% of the time during winter of anomalously high precipitation years. During winter of anomalously low precipitation years, precipitation only exceeds MPW 22% of the time. Thus, on average, there is roughly twice the number of days per winter season exceeding MPW during anomalously high precipitation than for anomalously low precipitation. Therefore, both an increase in MPW and an increase in dynamical convergence in the region are contributing to the anomalous precipitation at Alaskan stations and, in all likelihood, at Mt. Logan.

In combination, the daily pattern index, which shows that storms rather than blocking give rise to high accumulation, and the MPW, which demonstrates that high accumulation is associated with additional convergence, strongly suggest that increased moisture flux alone does not account for anomalous accumulation. Thus, the large-scale atmospheric patterns associated with anomalously high accumulation in the composite analyses arise from increased storminess.

6. Comparison with climate indices

Finally, it is of interest to compare the Logan accumulation time series with climate indices commonly used to describe Pacific and/or North Pacific climate variability. As shown in Table 3, direct correlations with these indices are quite low. As shown in section 5, precipitation station records in close proximity to each other do not correlate very highly with each other either, nor with the climate indices in Table 3. Clearly, there is a large amount of spatial variability within this region even when the entire region may be experiencing the same large-scale climate, such as a positive phase of the PNA. While these results argue against the Logan time series as a simple proxy for the ENSO or PDO index, for example, they do not imply that the Logan record does not usefully record North Pacific climate; one would not necessarily expect a time series influenced by nonlinear phenomena to correlate highly with any of the intrinsically linear climate indices listed in Table 3.

TABLE 3. Correlation coefficients (r) between Mt. Logan accumulation (column 2) and Yakutat precipitation (column 4) and four wintertime climate indices (for the period 1948–87 including the PDO, the PNA pattern, the Aleutian low pressure index (ALPI), and the Niño-3 index (Mantua et al. 1997; Wallace and Gutzler 1981; Beamish et al. 1997). Columns 3 and 5 indicate whether the correlations are significant at the 95% confidence level.

Climate indices	r (Mt. Logan)	95% Confidence	r (Yakutat)	95% Confidence
PDO	0.196	No	−0.034	No
PNA	0.242	No	0.266	No
ALPI	0.309	Yes	0.249	No
EI Niño-3	−0.036	No	0.110	No

We do note that, despite the low correlation between the Logan record and the PDO, the variance in either can be explained by an autoregressive process with the same 1-yr characteristic time scale. This supports recent theories for Pacific climate variability suggesting that wintertime reemergence of ocean mixed layer temperature anomalies from the previous winter can drive atmospheric variability (Alexander et al. 1999; Deser et al. 2003), and also highlights the point that “decadal” time-scale climate variability can be driven by physics with time scales that may seem surprisingly short.

7. Discussion

Our ability to place bounds on interannual climate variability and to characterize longer time-scale variability is largely contingent on extending the climate record beyond that of the instrumental record. Ice cores are one potential means to accomplish this, provided that reliable relationships can be demonstrated between climate variability and ice core parameters. For Mt. Logan, seasonal composites of the 500-hPa geopotential height and sea level pressure anomalies demonstrate a distinct relationship between wintertime atmospheric circulation and high accumulation. Specifically, the wintertime composites of high accumulation years show an enhanced trough–ridge structure at 500 hPa and sea level pressure over the northeast Pacific and western Canada, consistent with the PNA pattern. On the other hand, no statistically significant relationship can be demonstrated between atmospheric circulation for low or normal accumulation.

The nonlinear relationship between atmospheric circulation patterns and Logan accumulation rates reflects the particular atmospheric conditions required to produce anomalously high accumulation at this site. While the wintertime pattern of 500-hPa anomalies is consistent with increased southerly flow bringing in warmer, moister air and a deeper eastward-shifted Aleutian low during the winter season of high accumulation years, comparison between the composite patterns and daily anomaly patterns shows that both storms and blocking events project onto this pattern. Furthermore, comparison with precipitation station records from lower elevations indicates that most of the precipitation occurs during storms. Further comparison of maximum precipitable water with observed precipitation shows that

there is increased dynamical convergence associated with anomalously high accumulation. Together, these results suggest that individual storms, rather than either blocking events or a simple increase in mean flow, are responsible for high accumulation at Logan. Thus, the observed wintertime composite pattern for years with high accumulation is a necessary but insufficient explanation for those years. Normal and low accumulation years largely reflect the relative paucity of large storms, rather than any particular circulation anomaly pattern, and are therefore not a reliable indicator of circulation patterns. Comparisons between the accumulation and precipitation data, on the other hand, suggest that high accumulation at Logan is as reliable an indicator of large-scale atmospheric circulation as precipitation station records at lower elevations.

These results have important implications for the use of the Mt. Logan core in reconstructing climate and the interpretation of ice core accumulation records in general. In particular, we note that reconstruction of climate indices is usually based on assumptions of linear relationships between climate patterns and proxy indicators. Yet it is clear that the Mt. Logan accumulation record is better regarded as a direct indicator of wintertime North Pacific storminess rather than as an indicator of more generalized patterns or indices of climate variability. Indeed, the conclusion that anomalously high accumulation events are recorded quite faithfully at Logan is very encouraging from the point of view of climate reconstruction and illustrates the potential that ice cores offer in extending the climate record, even at rather high (i.e., interannual) frequencies, beyond that available in the instrumental record. The utility of the Logan record as a tool for reconstructing North Pacific climate, however, depends on the relationship between Northeast Pacific storms and broader-scale climate dynamics (e.g., Chang et al. 2002). It will thus be important when incorporating such records into climate reconstruction work to take into account the more complicated physics implied by these relationships. Finally, the spatial heterogeneity observed in comparing Logan with regional precipitation records reinforces the idea that a single proxy record is inadequate for quantitative climate reconstruction (e.g., Mann et al. 1998; Fisher 2002; Gedalof et al. 2002).

Acknowledgments. We thank Howard Conway, Greg Hakim, Nate Mantua, and Al Rasmussen for many help-

ful discussions that lead to the composition of this paper. We also thank Gerald Holdsworth for providing the Mt. Logan ice core data to the NGDC. Finally, we thank Gerald Holdsworth and an anonymous reviewer for constructive reviews that greatly improved the paper. This work was supported in part by the University of Washington Royal Research Fund.

REFERENCES

- Alexander, M. A., C. Deser, and M. S. Timlin, 1999: The reemergence of SST anomalies in the North Pacific Ocean. *J. Climate*, **12**, 2419–2433.
- Appenzeller, C., T. F. Stocker, and M. Anklin, 1998: North Atlantic Oscillation dynamics recorded in Greenland ice cores. *Science*, **282**, 446–449.
- Barlow, L. K., J. W. C. White, R. G. Barry, J. C. Rogers, and P. M. Grootes, 1993: The North Atlantic Oscillation signature in deuterium and deuterium excess signals from Greenland Ice Sheet Project 2 ice core. *Geophys. Res. Lett.*, **20**, 2901–2904.
- Beamish, R. J., C. E. Neville, and A. J. Cass, 1997: Production of Fraser River sockeye salmon (*Oncorhynchus nerka*) in relation to decadal-scale changes in the climate and the ocean. *Can. J. Fish. Aquat. Sci.*, **54**, 543–554.
- Bitz, C. M., and D. S. Battisti, 1999: Interannual to decadal variability in climate and the glacier mass balance in Washington, western Canada, and Alaska. *J. Climate*, **12**, 3181–3196.
- Blackmon, M. L., 1976: A climatological spectral study of the 500 mb geopotential height of the Northern Hemisphere. *J. Atmos. Sci.*, **33**, 1607–1623.
- Chang, E. K. M., S. Y. Lee, and K. L. Swanson, 2002: Storm track dynamics. *J. Climate*, **15**, 2163–2183.
- Deser, C., M. A. Alexander, and M. S. Timlin, 2003: Understanding the persistence of sea surface temperature anomalies in midlatitudes. *J. Climate*, **16**, 57–72.
- Elsberg, D. H., W. D. Harrison, K. A. Echelmeyer, and R. M. Krimmel, 2001: Quantifying the effects of climate and surface change on glacier mass balance. *J. Glaciol.*, **47**, 649–658.
- Fisher, D. A., 2002: High-resolution multiproxy climatic records from ice cores, tree-rings, corals and documentary sources using eigenvector techniques and maps: Assessment of recovered signal and error. *Holocene*, **12**, 401–419.
- , N. Reeh, and H. B. Clausen, 1985: Stratigraphic noise in time series derived from ice cores. *Ann. Glaciol.*, **7**, 76–83.
- Gedalof, Z., N. J. Mantua, and D. L. Peterson, 2002: A multi-century perspective of variability in the Pacific Decadal Oscillation: New insights from tree rings and coral. *Geophys. Res. Lett.*, **29**, 2204, doi:10.1029/2002GLO15824.
- Hodge, S. M., D. C. Trabant, R. M. Krimmel, T. A. Heinrichs, R. S. March, and E. G. Josberger, 1998: Climate variations and changes in mass of three glaciers in western North America. *J. Climate*, **11**, 2161–2179.
- Holdsworth, G., 1986: Evidence for a link between atmospheric thermonuclear detonations and nitric acid. *Nature*, **324**, 551–553.
- , H. R. Krouse, and M. Nosal, 1992: Ice core climate signals from Mount Logan Yukon 1700–1987. *Climate Since A.D. 1500*, R. S. Bradley and P. D. Jones, Eds., Routledge, 483–504.
- Jenkins, G. M., and D. G. Watts, 1968: *Spectral Analysis and Its Applications*. Holden-Day, 525 pp.
- Jensen, M. E., R. D. Burman, and R. G. Allen, 1990: Evapotranspiration and irrigation water requirements. *ASCE Man. Rep. Eng. Pract.*, **70**, 1–332.
- Kalnay, E., and Coauthors, 1996: The NCEP/NCAR 40-Year Reanalysis Project. *Bull. Amer. Meteor. Soc.*, **77**, 437–471.
- Lindzen, R. S., 1986: Stationary planetary-waves, blocking, and interannual variability. *Advances in Geophysics*, Vol. 29, Academic Press, 251–273.
- Mann, M. E., R. S. Bradley, and M. K. Hughes, 1998: Global-scale temperature patterns and climate forcing over the past six centuries. *Nature*, **392**, 779–787.
- Mantua, N. J., S. R. Hare, Y. Zhang, J. M. Wallace, and R. C. Francis, 1997: A Pacific interdecadal climate oscillation with impacts on salmon production. *Bull. Amer. Meteor. Soc.*, **78**, 1069–1079.
- Moore, G. W. K., G. Holdsworth, and K. Alverson, 2001: Extratropical response to ENSP as expressed in an ice core from the Saint Elias mountain range. *Geophys. Res. Lett.*, **28**, 3457–3460.
- , —, and —, 2002a: Variability in the climate of the Pacific Ocean and North America as expressed in the Mount Logan ice core. *Ann. Glaciol.*, **35**, 423–429.
- , —, and —, 2002b: Climate change in the North Pacific region over the past three centuries. *Nature*, **420**, 401–403.
- , —, and —, 2003: The impact that elevation has on the ENSO signal in precipitation records from the Gulf of Alaska. *Climatic Change*, **59** (1–2), 101–121.
- Nakamura, H., 1992: Midwinter suppression of baroclinic wave activity in the Pacific. *J. Atmos. Sci.*, **49**, 1629–1642.
- Overland, J. E., J. M. Adams, and N. A. Bond, 1999: Decadal variability of the Aleutian low and its relation to high-latitude circulation. *J. Climate*, **12**, 1542–1548.
- Paterson, W. S. B., 1994: *The Physics of Glaciers*. Reed Educational and Professional Publishing, 480 pp.
- Peixoto, J. P., and A. H. Oort, 1992: *Physics of Climate*. American Institute of Physics, 520 pp.
- Rosenberg, N. J., B. L. Blad, and S. B. Verma, 1990: *Microclimate*. 2d ed. John Wiley & Sons, 528 pp.
- Schmutz, C., J. Luterbacher, D. Gyalistras, E. Xoplaki, and H. Wanner, 2000: Can we trust proxy-based NAO index reconstructions? *Geophys. Res. Lett.*, **27**, 1135–1138.
- Schneider, T., and A. Neumaier, 2001: Algorithm 808: ARfit—A matlab package for the estimation of parameters and eigenmodes of multivariate autoregressive models. *ACM Trans. Math. Software*, **27**, 58–65.
- Trenberth, K. E., and J. W. Hurrell, 1994: Decadal atmosphere–ocean variations in the Pacific. *Climate Dyn.*, **9** (6), 303–319.
- Wallace, J. M., and D. S. Gutzler, 1981: Teleconnections in the geopotential height field during the Northern Hemisphere winter. *Mon. Wea. Rev.*, **109**, 784–812.
- Walters, R. A., and M. F. Meier, 1989: Variability of glacier mass balances in western North America. *Aspects of Climate Variability in the Pacific and Western Americas*, *Geophys. Monogr.*, No. 55, Amer. Geophys. Union, 365–374.
- Whitlow, S., P. Mayewski, J. Dibb, G. Holdsworth, and M. Twickler, 1994: An ice-core-based record of biomass burning in the Arctic and Subarctic, 1750 to 1980. *Tellus*, **40B**, 234–242.
- Zheng, J., A. Kudo, D. A. Fisher, E. W. Blake, and M. Gerasimoff, 1998: Solid electrical conductivity (ECM) from four Agassiz ice cores, Ellesmere Island NWT, Canada: High-resolution signal and noise over the last millennium and low resolution over the Holocene. *Holocene*, **8**, 413–421.